International Journal of Advanced Research in Physical Science (IJARPS)
Volume 4, Issue 2, February 2017, PP 28-36
ISSN 2349-7874 (Print) & ISSN 2349-7882 (Online)
www.arcjournals.org

Low Gravity Gas-Liquid Contactor: Effects of Reduced and Zero Gravity on Rayleigh-Plateau Instability

Raul Garcia-Sanchez, Janelle Holmes, Ajamu Abdullah, Aara'L Yarber, Ryan O'Donnell, Prabhakar Misra

Department of Physics and Astronomy, Howard University, Washington, DC, USA

Bradley Carpenter

NASA Headquarters, Washington, DC, USA

Abstract: *Liquids are incompressible fluids that move in response to applied forces. The dominant forces determining the shape of a free interface of a liquid at rest are gravity and surface tension. On Earth, at length scales larger than a few millimeters, gravity typically dominates. The purpose of this experiment was to observe the behavior of water, a Newtonian fluid, and the effects of surface tension, without the dominating force of gravity. During this experiment, multiple syringes of two different sizes were used to eject water during a microgravity flight experiment, forming a liquid column between two contact points. The behavior of this column was recorded and analyzed to determine the maximum length reached before the column breaks off. The longest water column size observed was 5.29 cm using a 3 ml syringe and 6.48 cm using a 10 ml syringe, respectively, under the reduced gravity experimental conditions aboard the modified Boeing 727 jet aircraft.*

Keywords: *Reduced Gravity, Microgravity, Water Column, Rayleigh-Plateau Instability*

1. Introduction

Simple liquids are incompressible fluids – they move in response to applied forces, but their density is essentially independent of pressure. The forces present in a liquid at rest (i.e. water in a cup) are due to the effects of gravity. Surface tension results from the fact that water molecules within the bulk liquid enjoy a lower energy state, due to their favorable van der Waals interactions with other water molecules, than do molecules at the interface between the bulk water and the atmosphere. It takes energy to create higher energy water molecules at the interface. This resistance to expanding the area of exposed surface is called surface tension. On Earth, gravity and surface tension both have roles in how liquids at rest behave. In large volumes, the weight of the liquid dominates the relatively small effect of surface tension. On small length scales, such as in capillaries, porous soils, and the droplets in ink jet printing, surface tension dominates over gravitational effects. In a free-floating space vehicle, gravity is essentially imperceptible, and surface tension is the dominant force determining the shape of a liquid at rest.

$$\text{Surface Area of Cylinder} = SA_{cyl} = 2\pi r^2 + 2\pi rh \quad (1)$$

$$\text{Surface Area of Sphere} = SA_{sph} = 4\pi r^2 \quad (2)$$

$$Vol_{cyl} = \pi r^2 h \quad (3)$$

$$Vol_{sph} = (4\pi r^3)/3 \quad (4)$$

For a given volume of water:

$$V_{cyl} = V_{sph} \quad (5)$$

$$\pi r^2 h = (4\pi r^3)/3 \quad (6)$$

Solving for h,

$$h = 4r/3 \quad (7)$$

Substituting h into (1) and simplifying we get

$$SA_{cyl} = (14\pi r^2)/3 \quad (8)$$

For some arbitrary r, let us say r= 0.13 cm, substitution into (1) and (2) yields

$$SA_{cyl} = 0.25\ cm^2$$

$$SA_{sph} = 0.21\ cm^2$$

Thus, to a good approximation

$$SA_{cyl} = SA_{sph} \quad (9)$$

Our research studies a classic phenomenon of surface shape instability due to surface tension, the Rayleigh-Plateau instability of a liquid cylinder under microgravity conditions. Rayleigh-Plateau instability has been widely studied and summarized [1-3]. The instability is a factor in areas including: inkjet printing, coating optical fibers for communication systems, enhanced oil recovery in pipelines, lab on a chip for performing laboratory functions and digital microfluidics, among others. Previous studies have been carried out to study a variety of compounds, such as liquid metals [4], metallic melts [5], and a variety of behaviors, such as the thermal conductivity of liquid materials [6], water droplet collisions [7] and cavitation [8], bubble splitting [9] and surface oscillation of droplets [10] have been investigated, all under microgravity conditions. Many of these studies have also been carried out in similar microgravity parabolic flight settings.

Liquid jets are good vehicles to study the effects of surface tension that arise due to cohesive properties of fluids. The hydrodynamic instability and singularity formation in liquid jet streams lead to drop breakups. Paradoxically, cohesive forces that give rise to surface tension are also the cause of breakup of the jet stream and are encountered in a wide array of applications, ranging from a variety of sprays for household and commercial use to industrial level jet engine technology. Besides their utility value, liquid jets serve as an ideal model probe for investigation of fundamental physical properties of fluids, such as surface tension, viscosity, and non-Newtonian rheology. The dynamics of a liquid jet can be readily influenced by turbulence and thermal excitation of the fluid, as well as by the characteristics of the surrounding fluid medium.

Rayleigh-Plateau instability clearly occurs as a result of surface tension acting on the air-liquid interface, and in our case, at the interface between the air and the water column. In the classical Rayleigh problem of the stability of an infinitely long liquid column the initial perturbations in the column shape, which are present due to random fluctuations, grow larger as the amplitude of the perturbations increases and the water column breaks down into droplets. Such perturbations can be considered to be made up of sinusoidal disturbances, some of which get enhanced over time, while other components decay over time. The growth and decay over time of a particular component is governed by its wavelength (directly proportional to the number of peaks and valleys formed per unit length) and the diameter of the parent cylindrical water column. It is the dominant constituent which grows at the fastest pace that will dictate the so-called pinching of the water column into droplets. These small perturbations on the surface of a liquid cylinder that reduce the diameter of the cylinder increase the pressure locally due to the force of surface tension. Liquid flows away from the region of reduced diameter in response to higher pressure, causing the diameter of the column to continue to shrink. Eventually the column will break up into droplets.

This experiment will be an introduction into free surface phenomena in gas-liquid interfaces under microgravity conditions using a gas-liquid contactor. In a microgravity environment the water column formed between the two contact disks will be significantly larger than one affected by gravity. The goal of this research was to determine the largest length (in cm) these water columns could reach before breakup. As the column gets longer and longer, additional modes of deformation of the column are possible. Eventually, in an ideal experiment the Rayleigh-Plateau instability will lead to the break-up of the water column. We used syringes of two different sizes in order to achieve a larger range of effective surface tension.

2. Materials and Methods

An 80/20 frame and polycarbonate sheets were used to support the syringe, plunger, and cameras for the investigations. Syringes of two different sizes, 3 mL and 10 mL, were fitted into the plunger; and pressing the handle of the plunger deployed a liquid column between the two plates. Table 1 shows the type of syringes that were used for the experiment.

Table1. *Syringe types and sizes*

Type	Syringe Volume (ml)	Water Volume (ml)
1	3	3
2	10	3-5
3	10	10

The first plate is fixed at the tip of the syringe, while the second slides with the plunger, allowing the team to vary the length of the column. Upon entering free fall, a team member deployed the water column to a length per the experiment test matrix. The other teammates observed the column for 5-10 seconds to determine the stability of the column. If the column was not disrupted, the deployed water was drawn back into the syringe. If the column was disrupted, air and water was drawn into the syringe to deploy a column of an air-water mixture. Figure 1 shows the schematic for the side view of the liquid-gas contactor apparatus. Table 2 shows the materials used to construct the liquid-gas contactor apparatus.

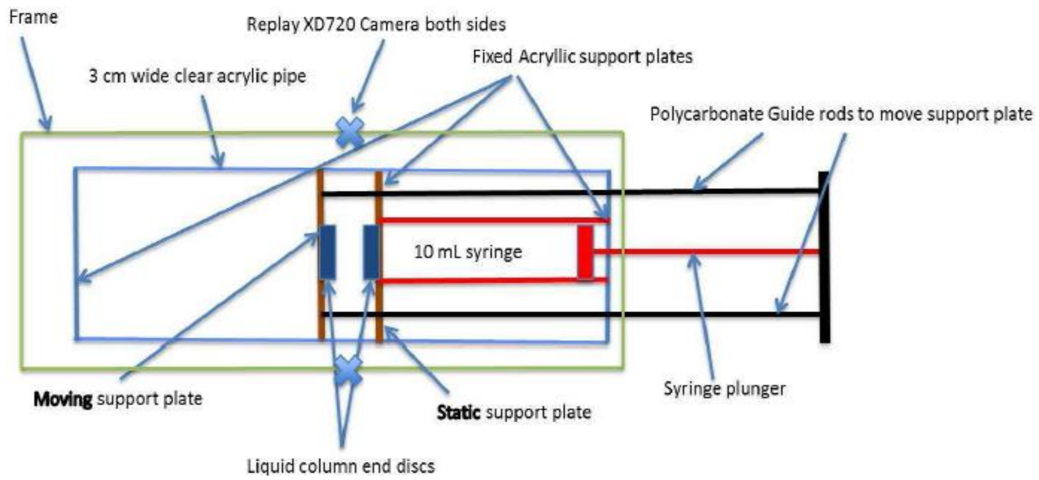

Figure1. *Schematic of the apparatus*

Table2. *Liquid-Gas Contactor Parts*

Description	Amount	Dimensions (in) (L x W x H)	Weight (lbs)
Quickframe #9030: Double Twin Flanged	12	Rectangular parallelepiped 12 x 1 x 1 0.5-size Flange	5.11
QuickframeCorners#9250 3-way corner	8	Network of Cubes 4 x 4 x 3.48	0.640
Replay XD720 Cameras	2	Cylinder 3.2 x 0.9	0.250
¼” Thick Impact-Resistant Polycarbonate Sheet	6	Sheet 12 x 12 x ¼	9.72
Impact-Resistant Polycarbonate Rods	3	Cylinder ($V=Pi*r^2*l$) (l) 4.0 x (r) 0.125	0.03
Syringes (3ml and 10ml)	1	-	0.3
Impact-Resistant Polycarbonate Round- Tubes	1	Hollow Cylinder ($V=Pi*r^2*l$) (l) 12 x (r)0.6259	0.51

There were two microgravity flights on November 12-13 during the flight week (November 8-15, 2013) that served as the experimental backdrop for this research. Both flights occurred as part of the NASA Microgravity MUREP program [11]. The airplane (see Figure 2(a)) used for the experiments was a three-engine Boeing 727-200F adapted for microgravity tasks. The microgravity conditions were achieved by flying the plane through a sequence of parabolic trajectories (see Figure 2(b)), which resulted in brief periods of less than one “g” acceleration. Each parabola was initiated with a 1.8-g pull-up and terminated with a 1.8-g pull-out (Figure 2(b)). Initially, the airplane flies level at 20,000+ feet, then gradually increases the angle of the aircraft to 45° and gains in altitude. Following the increase in altitude, the aircraft is leveled once more to simulate a microgravity-like environment in which the passengers in the plane experience a low gravity pull and are weightless for about 30 seconds. The plane then goes through a 45° descent in altitude. This maneuver is repeated several times and each time a stable water column was attempted.

(a) 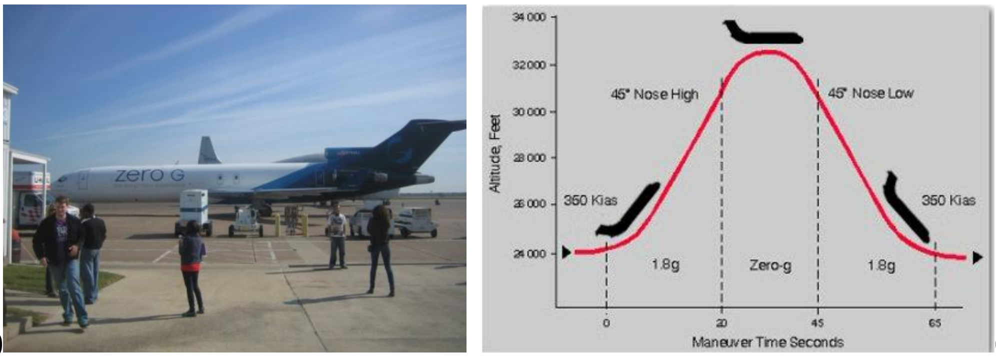 (b)

Figure2. (a) *Zero-G airplane used for the experiments, sitting on the tarmac at Ellington Field, Houston, TX, prior to the flight; and* **(b)** *the microgravity flight trajectory [12].*

Two groups, each composed of two students and one mentor, participated in two separate flights on November 12 and November 13, 2013, respectively. Two of the crewmembers (henceforth, Crewmember 1 and Crewmember 2) took positions holding the ends of the experiment frame, while the third crewmember (henceforth, Crewmember Three) grasped the frame and pushed/pulled the syringe handle. Upon entering free fall, Crewmember Three deployed the water column to a length per the experiment test matrix, while Crewmembers One and Two observed the water column and confirmed that the water column was properly formed. The column was observed for 5-10 seconds, depending on environmental conditions of the airplane flight and the speed at which the contact points separated, to determine the stability of the column. The behavior of the column was recorded using a pair of video cameras (Replay XD720 at 30 frames/sec) mutually orthogonal to one another. Once the column started wobbling and broke off at the contact points, the final measurement on the length at the time this occurred was catalogued. The syringe was replaced with a new one after each free-fall parabola. These measurements continued on level flights until the series of parabolas were completed .

3. Results and Discussion

The first flight consisted of 29 parabolas and the second one consisted of 20 parabolas. Various microgravity conditions, including Mars (0.38g) and Moon (0.15g) gravity, were simulated. Team 1 produced 15 well-defined water columns and team 2 produced 14 water columns. Table 3 (and Figure 3) and Table 4 (and Figure 4) show the water column data values gathered by Team 1 and Team 2, respectively.

Table3. *Water column sizes (cm) for Team 1*

Parabola #	Syringe Type	Water Volume Used (ml)	Water Column Length (cm)	Water Column Width (cm)
1	1	1.0	2.91	1.32
2	1	0.5	2.38	1.45
5	1	1.0	2.51	1.59
6	1	1.0	2.91	1.59
7	1	1.25	3.31	1.45
7.5	1	1.0	2.91	1.77
10	1	1.0	2.91	1.59
13	1	0.8	2.65	1.45
14	1	1.0	2.91	1.59
17	2	5.0	5.29	2.64
24	1	0.5	2.65	1.45
25	1	1.0	2.38	1.45
25.5	1	2.0	3.31	1.77
26	1	1.0	2.83	1.45
27	1	1.0	2.91	1.45
27.5	1	2.5	4.23	1.77
28	2	5.0	4.68	1.98
29	2	4.0	4.23	2.12

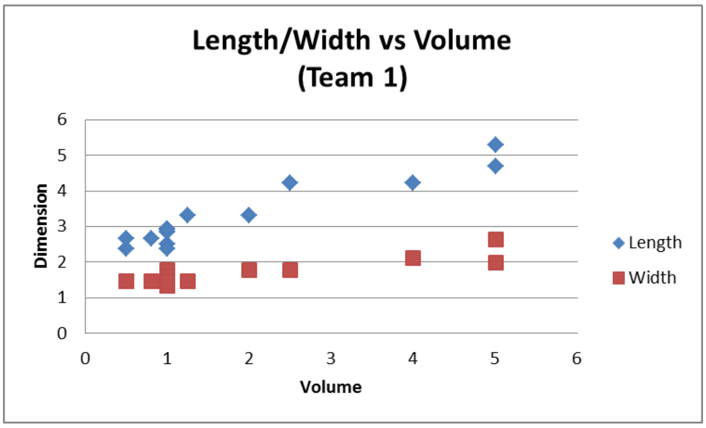

Figure3. *Plot of water column dimensions (cm) vs volume (ml) used for Team 1*

Table4. *Water column sizes (cm) for Team 2*

Parabola #	Syringe Type	Water Volume Used (ml)	Water Column Length (cm)	Water Column Width (cm)
2	3	5.0	6.48	2.38
4	3	4.0	5.02	2.64
6	3	4.5	5.82	2.51
7	3	4.5	4.50	2.25
8	3	4.0	3.04	2.51
9	3	3.0	3.17	2.25
11	3	3.5	4.63	2.38
12	3	2.5	4.23	2.38
14	3	5.0	5.82	2.78
15	1	0.5	2.64	0.92
17	1	1.0	3.70	1.45
18	1	1.0	3.57	1.32
19	3	3.0	4.37	2.38
20	3	4.0	5.56	2.38

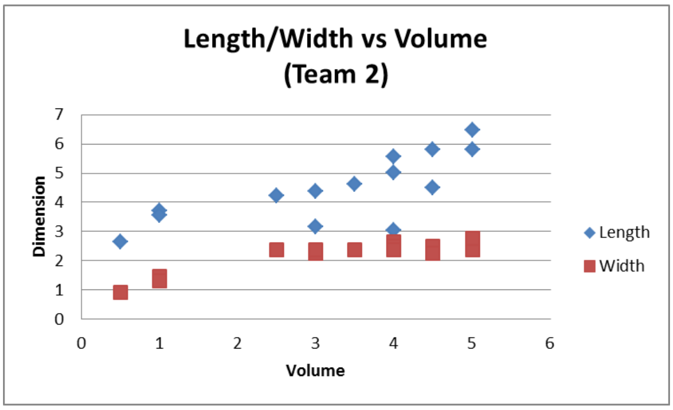

Figure4. *Plot of water column dimensions (cm) vs volume (ml) used for Team 2*

Table 5 summarizes the special cases observed during both flight experiments and their respective behavior.

Table5. *Water columns that exhibited special behavior*

Team	Parabola #	Behavior
1	7-7.5	Column Reformation
1	9	Droplet Wobbling
1	17	Whirlpool Effect
1	21	Column Wobbling
1	25-25.5	Column Reformation
1	27-27.5	Column Reformation
1	28	Droplet Bridging
2	4	Droplet Bridging

A. Column Reformation

Of the various columns studied, the columns labeled twice (i.e. 7 and 7.5) refer to columns which initially broke off, but then proceeded to remerge after the two droplets attached to each contact disk came together. Figure 5 shows the frame-by-frame behavior of Team 1's Column 7, which is one of the columns that underwent column reformation.

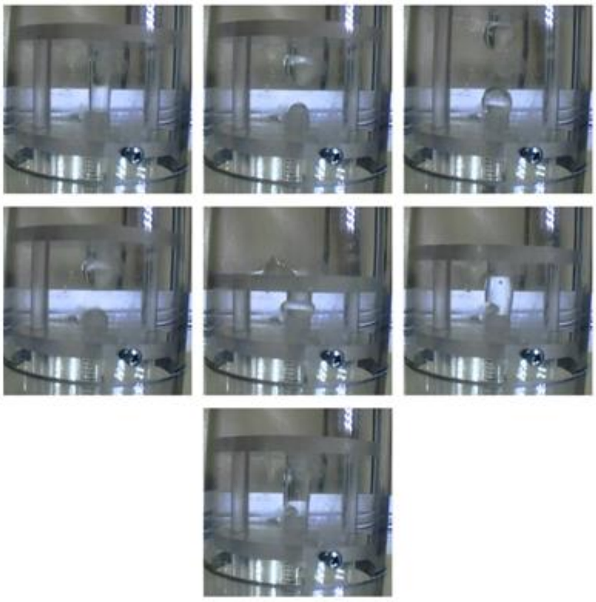

Figure5. *Frame-by-Frame display of Team 1's Column 7 during reformation*

This effect is similar to the attraction force scenario that was observed for some columns. In this case, however, rather than keeping the contact disks separate enough, they are brought down all the way to reform the broken column. In all the cases that this "column reformation" effect was observed, the second column formed was larger than the original, likely due to the fact that more water was pushed out of the syringe as the contact disks separate a second time. This effect was observed three times in Team 1's flight experiment on Column 7, 25 and 27.

B. Droplet Wobbling

This effect occurs when the water expelled out of the syringe is left on the surface of the lower contactor disk without making contact with the upper disk. The microgravity effect causes the droplet to remain stuck to the disk, rather than breaking off the disk, and the droplet begins to wobble as a result of the airplane vibrations. This effect occurred most predominantly in Team 1's Column 9, though it was also observed for other columns. Since no columns were formed from these attempts, they are not labeled in Tables 3 & 4. Figure 6 shows the frame-by-frame of Team 1's column attempt 9, which shows this "droplet wobbling" effect in action.

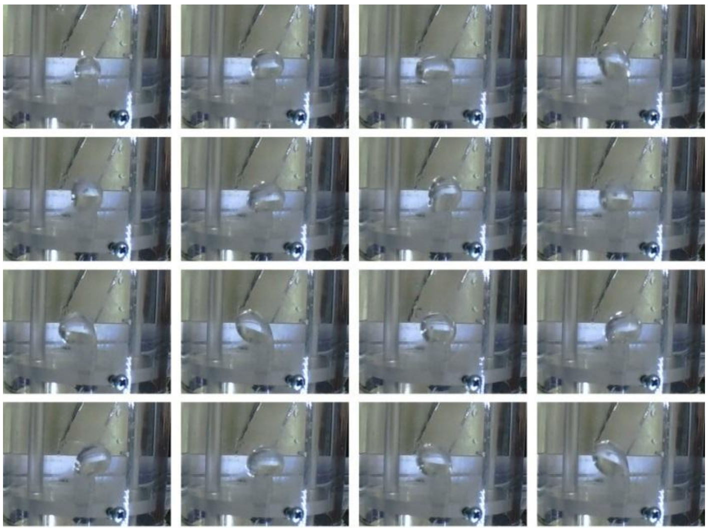

Figure6. *Frame-by-Frame display of Team 1's Column 9 formation illustrating droplet wobbling observation (time evolution from left to right row-wise)*

C. Column Wobbling

This effect occurs when the column is small enough that it cannot be broken as a result of the Rayleigh-Plateau effect. In this situation, the Rayleigh effect occurs, causing the column to wobble from side to side, but due to the microgravity environment and the small size of the column, it does not provide enough force to overcome the surface tension force from the water on the disks. Figure 7 shows this "column wobbling" effect frame-by-frame.

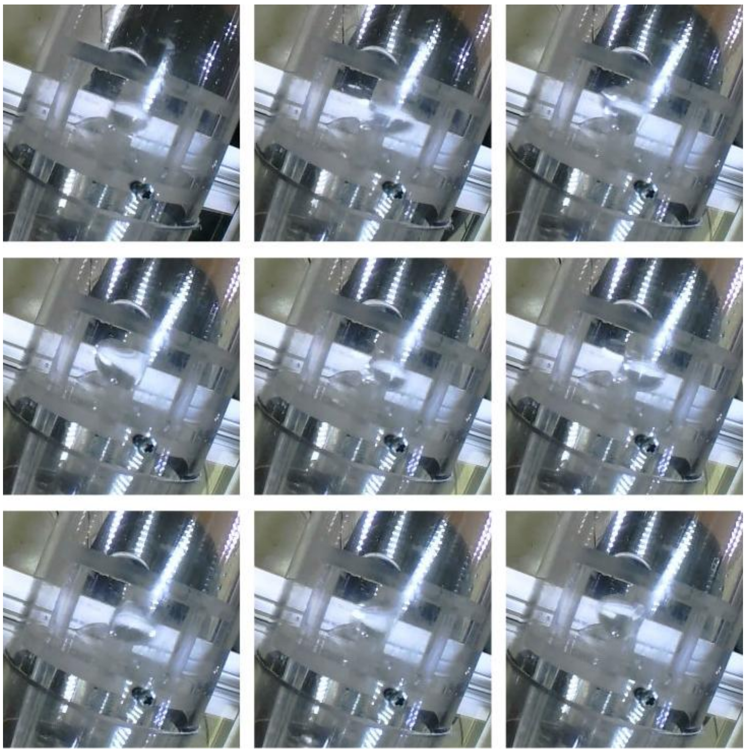

Figure7. *Frame-by-Frame display of Team 1's Column 21 illustrating the column wobbling effect (time evolution from left to right row-wise)*

D. Whirlpool Effect

This effect occurs as a result of early severe wobbling as the column forms. The wobbling force travels upward with the column as it extends, giving it a disproportionate width, forming a tornado/whirlpool-like effect on the column. Figure 8 shows the "whirlpool effect" during column attempt 17 for Team 1.

Figure8. *Frame-by-Frame display of Team 1's Column 17 showing the whirlpool effect (time evolution from left to right row-wise)*

E. Droplet Bridging

This effect occurs when the upper contactor disk comes close enough to make momentary contact with a water droplet on the surface of the lower contactor disk. It causes the water droplet to be "pulled" into the upper contactor disk, creating a bridge between them and therefore a water column. This "droplet bridging" effect was observed once by each group and was the only effect observable by both groups.

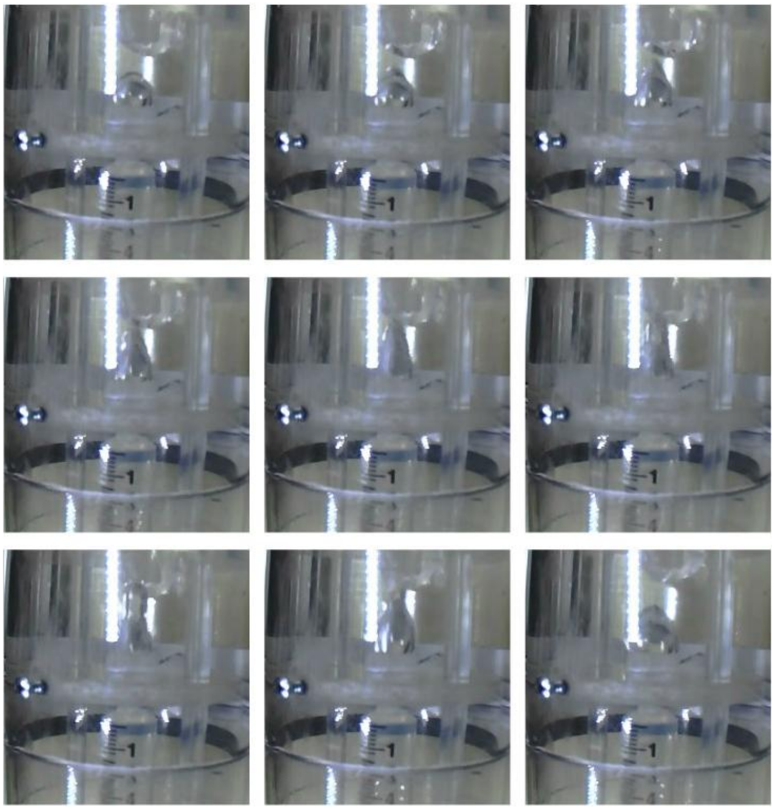

Figure9. *Frame-by-Frame depiction of Team 2's Column 4 illustrating the observed droplet bridging effect (time evolution from left to right row-wise)*

4. CONCLUSIONS

We were able to observe a wide range in the quality and size of the water columns formed by both groups. Of these, we found that the largest producible water column was 5.29 cm using a 3 ml syringe and 6.48 cm using a 10 ml syringe. In addition to the length, we were also able to determine the width of the water columns. Overall, we found that the length of the water column using the 3 ml syringe ranged from 2.39-2.91 cm and its width ranged from 1.32-1.77 cm when using 1.0 ml of water, which was the most common volume occurrence; whereas using a 10 ml syringe, we were unable to generate enough reproducible columns using the same volume of water enough times to reach a conclusion. We can also discern from Tables 3 and 4 that when the amount of liquid water used to generate a water column was the same for both groups, Team 2's column lenght were larger, which is a result of the bigger bore size of the 10 ml syringe. From Figures 4 and 5, we observe that the width does not change much with increasing water volume and is likely related to the bore size of the syringe and the size of the contact disks.

We observed five clear effects of microgravity on the water column, namely column reformation, droplet wobbling, column wobbling, whirlpool effect, and droplet bridging, as illustrated in Figures 5-9, respectively. We observed the behavior of water in droplet and column formation as a side-effect of the unstable microgravity environment that the liquid-gas contactor device was subjected to. In addition to the formation of regular water columns, we also observed a variety of interesting effects that occurred on the water column under different conditions (i.e. syringe plunging to disk movement ratio, shaking, syringe size, etc.). While the column and droplet wobbling examples listed above are perhaps due to the shaking that the gas-liquid contacor experiences during the parabolic trajectories, in a perfectly stable microgravity environment, it is likely that the wobbling forces that caused some of the effects observed may not occur at all.

There were some issues regarding the lighting from the airplane lights obscuring some of the visibility of the columns but not to the point where it was not possible to measure the water columns. Some of the effects we had to deal with, such as the shaking from the airplane due to turbulence, made it difficult to form water columns on every attempt. Overall, the success rate of water column formation was roughly 51% for Team 1 and 70% for Team 2.

ACKNOWLEDGEMENTS

The authors would like to thank the *Reduced Gravity Education Flight Program* for the research opportunity and travel grant support, and the NASA Johnson Space Center, especially the staff and Zero-G flight crew at Ellington Field, Houston, TX. We would also like to thank the Office of the Dean, College of Arts & Sciences, and the Department of Physics & Astronomy, Howard University, for their support, as well as the Support Staff and Machinists from the Departments of Mechanical Engineering and Physics & Astronomy for their help in assembling the liquid-gas contactor.

REFERENCES

[1] Sharp D.H., An overview of Rayleigh-Taylor Instability, Physica 12D, 3-18 (1984).

[2] Papageorgiou D.T., On the breakup of viscous liquid threads, Phys. Fluids 7, 1529-1544 (1995). http://dx.doi.org/10.1063/1.868540.

[3] Miyamoto U., “Curvature Driven Diffusion, Rayleigh–Plateau, and Gregory–Laflamme,” Phys.Rev.D 78, 026001 (2008).

[4] Egry I., Lohoefer G., Schwartz E., Szekely J. and P. Neuhaus, Surface Tension Measurements on Liquid Metals in Microgravity, Metallurgical and Materials Transactions B, Volume 29b, 1031 (1998).

[5] Egry I., Jacobs G., Schwartz E. and Szekely J., Surface tension measurements of Metallic Melts under Microgravity, International Journal of Thermophysics, Volume 17, Issue 5, 1181-1189 (1996).

[6] Nagai H., Rossignol F., Nakata Y., Tsurue T., Suzuki M. and Okutani T., Thermal conductivity measurement of liquid materials by a hot-disk method in short-duration microgravity environments, Materials Science and Engineering: A, Volume 276, Issues 1–2, 15, 117–123 (2000).

[7] Suñol F., and González-Cinca R., Droplet collisions after liquid jet breakup in microgravity conditions, J. Phys.: Conf. Ser. 327 012026 doi:10.1088/1742-6596/327/1/012026 (2011).

[8] Kobel P., “Cavitation Studies in Microgravity,” 38th COSPAR Scientific Assembly (2010).

[9] Yoshikawa H.N., Zoueshtiagh F., Caps H., Kurowski P. and Petitjeans P., Bubble splitting in oscillatory flows on ground and in reduced gravity, Eur. Phys. J. E 31, 191–199. DOI 10.1140/epje/i2010-10561-y (2010).

[10] Fujii H., Matsumoto T. and Nogi K., Analysis of Surface Oscillation of Droplet Under Microgravity for the Determination Of its Surface Tension, Acta Materialia, 48 (11), 30, 2933–2939 (2000).

[11] Interface Control Document Boeing 727-200 Zero Gravity Corporation, December 2008, Revision A2.

[12] https://jsc-aircraft-ops.jsc.nasa.gov/Reduced_Gravity/trajectory.html